Journal of Engineering Science and Technology
Vol. 17, No. 2 (2022) 1561 - 1576
© School of Engineering, Taylor's University

SOLAR IRRADIANCE FORECASTING USING KERNEL EXTREME LEARNING MACHINE: CASE STUDY AT LAMONGAN AND MUARA KARANG REGIONS, INDONESIA

MUHAMMAD ABDILLAH[1,*], WAHYU AGUNG PRAMUDITO, TEGUH ARYO NUGROHO[1], DINA NURUL FITRIA[2,3]

[1]Department of Electrical Engineering, Universitas Pertamina, Indonesia
[2]Department of Economics, Universitas Pertamina, Indonesia
Jalan Teuku Nyak Arief, Simprug, Kebayoran Lama, Jakarta 12220
[3]Principal of Amina Research and Business Consulting, Indonesia
*Corresponding Author: m.abdillah@universitaspertamina.ac.id

Abstract

Nowadays, many countries focus on developing clean energy such as photovoltaic (PV) as public awareness to degrade global warming has increased. However, PV power output is intermittently affected by weather conditions. Therefore, an advanced method is required to predict solar irradiance to obtain the precise PV output. This paper proposed a method called kernel extreme learning machine (K-ELM) used to forecast solar irradiance. Solar irradiance is very important in planning and operating of PV generation system to reduce procurement costs and improve the quality and safety of PV output to supply the load. The meteorological and solar irradiance data utilized for the K-ELM model were taken from the Lamongan and Muara Karang areas, Indonesia. The mean absolute error (MAE) criterion was employed to measure the accuracy of the proposed method. From the simulation results, the proposed K-ELM gained the best performance with 0.6669, and 0.791 for MAE in the Lamongan and Muara Karang regions, respectively. The ELM attained the second-best results for MAE with 0.807 and 0.8001. The LS-SVM obtained the third results for MAE with 1.2492 and 1.4315. The performance of SVM is the least with 4.9829 and 4.6398 for MAE in the Lamongan area and Muara Karang region, respectively.

Keywords: ELM, K-ELM, Photovoltaic, LS-SVM, SVM.

1. Introduction

Indonesia is the largest archipelago in the world that consists of 17.000 islands. Moreover, Indonesia has a population estimated at 269.54 million in 2019. Since Indonesia lies on the equator line, it has many advantages where almost all areas in this country receive direct solar light over the years. To date, this country is also endowed with rich natural resources included water, solar light, wind, geothermal, and other natural resources that are utilized as renewable energy (RE) sources [1]. The need and necessity of adequate energy harvested from natural resources for multiple goals have been revealed by most of the researchers in the global sector for decades. The blessing of solar light possessed by almost all areas in Indonesia had encouraged many researchers to develop an advanced RE technology as a solution to energy problems by harvesting energy from solar light, which is naturally replenished.

The advanced technology equipment that can harvest energy from solar light is called a photovoltaic (PV) panel, which collects solar light by utilizing solar cells as components of a PV panel and converting it into electric power. However, the power output of PV panels is highly dependent on solar irradiance. The solar irradiance process is a complex issue in nature because its magnitude is affected by the amount of various climatological and aerial components such as temperature, relative humidity, wind speed, and others [2, 3]. Moreover, the measurement of solar irradiance in nature is an arduous issue [4]. For decades, the empirical model was computed manually with several boundaries, including a case study of distinctive behaviours/patterns and diversity in the results, since the high stochasticity is included in actual data [5, 6]. The solar irradiance predictions are classified into three categories, which are; intra-hour prediction, short-term prediction, and long-term prediction. The intra-hour prediction has an hourly time horizon, while short-term prediction has a daily time horizon. The long-term prediction may have weeks or months or even years of time horizon. In a meantime, researchers in the energy sector are driven to construct a new method to forecast solar irradiance with high accuracy. The objective is to reduce the need for PV panels and the cost of installation economically and efficiently.

Since G. Mihalakakou has successfully proposed a neural network (NN) in order to forecast the solar irradiance [7], the prediction of solar irradiance based on an intelligent approach has gained the attention of many researchers in renewable energy fields. Numerous models to predict the solar irradiance using AI have been developed, such as adaptive neuro-fuzzy inference systems (ANFIS) [8], artificial neural network (ANN) [9], extreme learning machines (ELM) [10], long-short term memory (LSTM) [11], ANN-based corrective algorithm [12], hybrid evolutionary neural networks [13], hybrid artificial neural network and principal component analysis [14], convolutional long short-term memory [15], and deep neural networks [16]. In most cases, these approaches are very good for prediction, but some are more subjective in selecting parameters. In addition, these learning methods require an iterative process for their learning phase, so they are generally slow.

This paper proposes a kernel extreme learning machine (K-ELM) to forecast solar irradiance. The proposed method has some advantages in terms of fast learning speed and good generalization performance. Also, it has been applied in many fields such as condition monitoring [17], automatic heartbeat classification [18], prediction of COVID-19-pneumonia [19], prediction of heavy metals removal by biochar [20],

fault diagnosis of aircraft engine [21], fault diagnosis of high-voltage circuit breakers [22], node localization in wireless sensor networks [23], and wind power prediction [24]. In this paper, the meteorological and solar irradiance datasets were collected from Lamongan and Muara Karang areas because both areas are coastal areas that have high solar irradiance over the years. The learning algorithm proposed in this study is compared to standard ELM, SVM, and LS-SVM.

2. Kernel Extreme Learning Machine

An ELM is a new kind of machine learning algorithm (MLA) [25]. The ELM model utilizes a feed-forward neural network with a single hidden layer. The input and output data are mapped quickly by this learning algorithm [26].

The ELM approach is employed to tackle the drawback of traditional neural networks (NN) [27] in terms of learning speed. A conventional NN requires a longer learning time since its network parameter is determined iteratively and more training samples must be included to obtain predictive output accurately [28].

The learning time of ELM is faster than the standard neural network because there is no iteration required in ELM. However, ELM has a weakness; that is trial-and-error method employed to calculate neuron in the hidden layer of ELM. Furthermore, the hidden layer in the ELM method needs more neurons to provide better prediction results. Hence, the weighting parameter of ELM is selected randomly. The data from input layer to hidden layer of ELM is converted using the kernel function into higher dimensional feature subspaces. This method aims to transform a non-linear to a linear pattern. Additionally, it is utilized to reduce computational time for its learning process.

Given N data samples $\{(x_i, t_i)|x_i \in R^n, t_i \in R^m, i = 1, \dots, N\}$, the mathematical model of ELM output with M hidden neurons is formulated using Eq. (1) [21],

$$y_M(x) = \sum_{i=1}^{M} \beta_i h_i(x) = h(x)\beta \tag{1}$$

The objective of ELM learning algorithm is to minimize the training error and the output weight at the same time as defined in Eq. (2) [24].

$$\text{Minimize: } \|H\beta - T\|, \|\beta\|. \tag{2}$$

The problem of Eq. (2) could be solved by using the Karush-Kuhn-Tucker optimality condition as defined in Eq. (3) [29].

$$\beta = H^T \left(\frac{1}{C} + HH^T \right)^{-1} T \tag{3}$$

The output of ELM in Eq. (4) is obtained by solving the formulation of β in Eq. (3) and substituted to Eq. (1) [29].

$$y(x) = h(x)H^T \left(\frac{1}{C} + HH^T \right)^{-1} T \tag{4}$$

The Mercer's condition utilized as kernel method which is defined in Eq. (5) is employed to overcome the unknown of feature mapping $h(x)$ [20].

$$O = HH^T : m_{ij} = h(x_i)h(x_j) = \Omega(x_i, x_j) \tag{5}$$

Thus, the output function $y(x)$ of K-ELM is represented in Eq. (6) [19].

$$y(x) = \left[\Omega(x, x_1), \mathrm{K}, \Omega(x, x_M)\right]\left(\frac{1}{C} + O\right)^{-1} T \tag{6}$$

Many kernel functions satisfying the Mercer condition are available from the existing literature, such as the linear kernel, radial basis function kernel, polynomial kernel, Gaussian kernel, and exponential kernel. In this research work, a radial basis function (RBF) based kernel as defined in Eq. (7) is employed to test the performance of the proposed method [18].

$$\Omega(x, y) = \exp\left(\frac{\|x - y\|^2}{2\sigma^2}\right) \tag{7}$$

The K-ELM parameters (C and σ) have a great effect on the performance of the proposed algorithm. Therefore, these parameters should be properly chosen. The proposed learning algorithm proves to be more stable than conventional ELM and faster in process computing compared to SVM [30, 31]. The network scheme of K-ELM approach is depicted in Fig. 1.

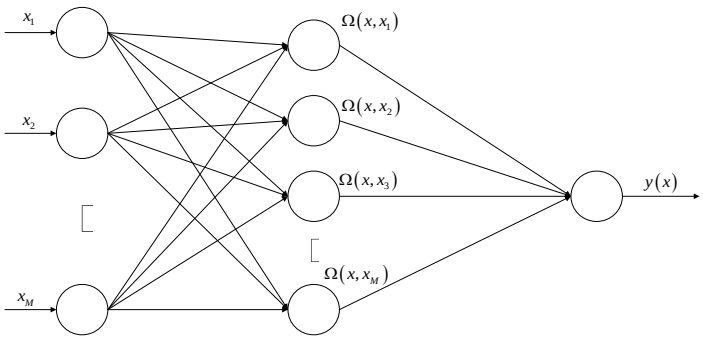

Fig. 1. Network scheme of K-ELM method.

3. The Implementation of The Proposed Method

The features selected as input data of K-ELM as shown in Fig. 2 consist of temperature (C), wind speed (m/s), and humidity (%). As the predicted data or the output of K-ELM, solar irradiance (kWh/m^2/day) data is utilized. The procedures for the solar irradiance forecasting model are classified into the training process and the testing phase.

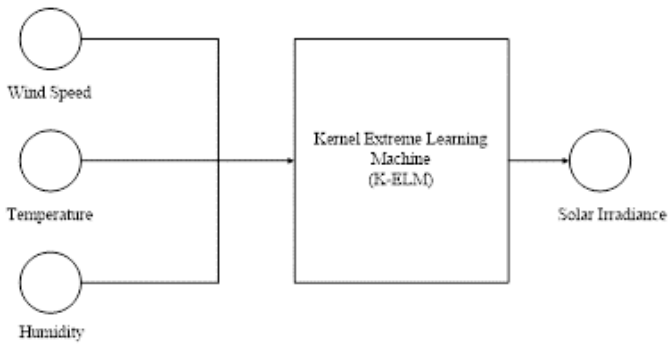

Fig. 2. Proposed K-ELM scheme.

The procedures for the training phase of the K-ELM method can be described as follow:

i. Collect the data of wind speed, temperature, humidity, and solar irradiance.

ii. Utilize wind speed, temperature, and humidity as input data for K-ELM. The output data of K-ELM is the predicted solar irradiance.

iii. Normalize the real record value of input and output data of K-ELM to [-1,1]. The normalization of the datasets of wind speed, temperature, humidity, and solar irradiance is conducted because their real data records have a large value difference. The maximum and minimum values of wind speed, temperature, humidity, and solar irradiance are depicted in Table 1. The patterns of wind speed, temperature, humidity, and solar irradiance are shown in Figs. 3(a)-(b). The mathematical model for data normalization is described in Eq. (8).

$$X_n = 2(X_p - X_{p\text{-}min}) / (X_{p\text{-}max} - X_{p\text{-}min}) - 1 \tag{8}$$

The minimum and maximum values ($X_{p\text{-}min}$ and $X_{p\text{-}max}$) of wind speed, temperature, humidity, and solar irradiance are illustrated in Table 1.

iv. Convert the input data of K-ELM using RBF kernel in Eq. (7) into high dimensional features.

$$\Omega(x, y) = \exp\left(\frac{\|x - y\|^2}{2\sigma^2}\right)$$

The kernel function is utilized to substitute the hidden neuron in the conventional ELM. RBF kernel is the most generalized form of kernelization and one of the most widely used kernels due to its similarity to the gaussian distribution.

v. Set the parameters of K-ELM (i.e. C and σ).

vi. Simulate the training stage using Eqs. (2)-(5) to produce the forecasted data of K-ELM in Eq. (6).

vii. Denormalize the predicted result or output data of K-ELM to their exact values using Eq. (9). In this stage, the predicted result in the range of value [-1, 1] is transformed into their exact value.

$$X_d = 0.5(X_p + 1) \text{ x } (X_{p,max} - X_{p,min}) + X_{p,min} \tag{9}$$

viii. Compute the accuracy of the predicted result. Statistical indicator namely mean absolute error (MAE) as depicted in Eq. (10) is employed for measuring the performance of the proposed method.

$$MAE = \frac{\sum_{i=1}^{N} |y_i - y_i|}{N} \tag{10}$$

ix. If the MAE value is minimum, save the K-ELM parameters (i.e. C and σ) obtained from the training stage for the next step (testing process) and print out the predicted data of solar irradiance. Otherwise, go to step 5 until the minimum of MAE is obtained.

After the training phase has been conducted, the next procedure is the testing phase for the K-ELM approach to obtain the predicted value of solar irradiances. The workflow of the testing stage is described as follows:

i. Prepare the data for the testing phase (i.e. wind speed, temperature, humidity, and solar irradiance).
ii. Use wind speed, temperature, and humidity as input data of K-ELM. Solar irradiance is employed as the forecasted data of K-ELM.
iii. Utilize the K-ELM parameters (i.e. C and σ) obtained from the training stage.
iv. Normalize the input and output data of K-ELM to [-1,1] using Eq. (8).
v. Convert the input data of K-ELM using RBF kernel function Eq. (7) into high-dimensional features.
vi. Compute the predicted data of K-ELM using Eq. (6).
vii. Denormalize the predicted data of K-ELM from [-1, 1] to their exact value using Eq. (9).
viii. Compute the degree of accuracy for K-ELM output based on MAE using Eq. (10).
ix. Print out the predicted solar irradiance.

4. Results and Discussion

4.1. Forecasting data model and statistics for evaluation

To develop the proposed forecasting method, we utilized the real meteorological and solar irradiance data from Lamongan and Muara Karang areas, Indonesia, which were downloaded from the website of NASA prediction of worldwide energy resource [32]. The real data measurements were recorded from January 1st, 2013, to April 30th, 2019 (5 years and 4 months). The simulation process of this research work is conducted by AMD Ryzen 7 with 3.20 GHz. The proposed prediction method was written using MATLAB 2014a software [33]. In this research work, the dataset model was classified into the training and testing datasets. The meteorological and solar irradiance data aforementioned in section 3 were employed for training and testing phases. The datasets from January 1st, 2013, to December 31st, 2018 (2191 days) were included for the training process. The meteorological and solar irradiance data collected from January 1st, 2019, to April 30th, 2019 (120 days) were included as testing datasets. The patterns of meteorological and solar irradiance datasets of Lamongan and Muara Karang regions for 5 years and 4 months are shown in Fig. 3, while their maximum and minimum values are listed in Tables 1 and 2. The level of wind speed, temperature, humidity, and solar irradiance in Lamongan is higher than in Muara Karang.

Table 1. Maximum and minimum values of datasets in Lamongan.

	Wind speed (m/s)	Temperature (C)	Humidity (%)	Solar Irradiance (kWh/m^2/day)
max	7.12	31.19	95.32	7.47
min	0.43	22.69	43.64	0.58

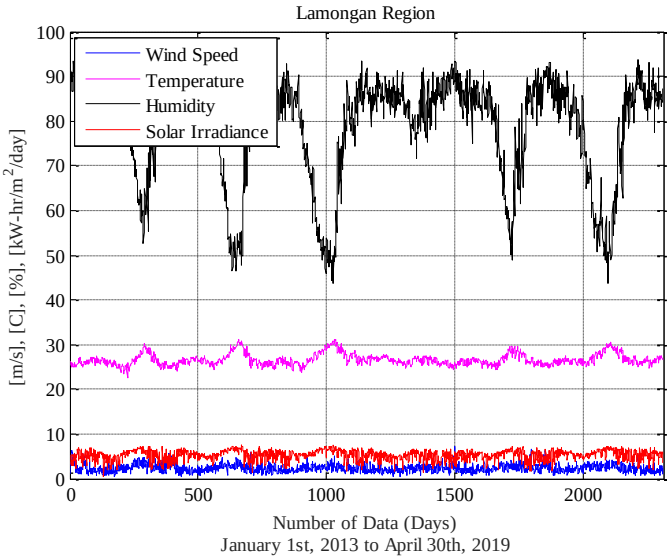

(a) Lamongan.

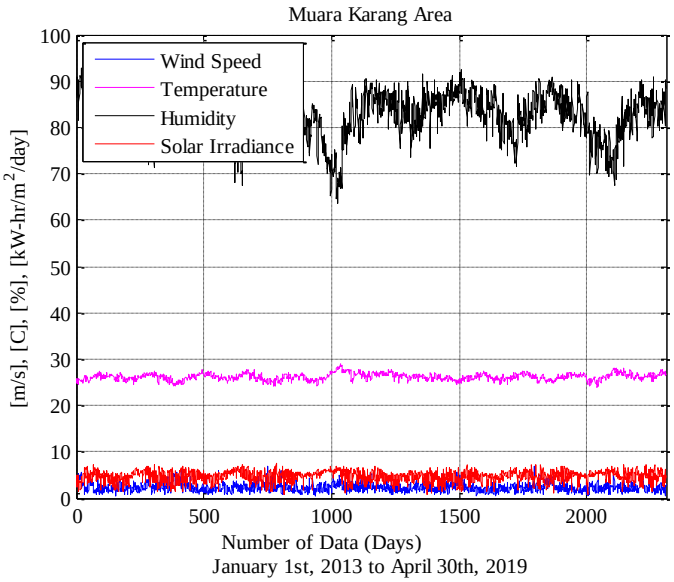

(b) Muara Karang.

Fig. 3. Meteorological and solar irradiance datasets.

Table 2. Maximum and minimum values of datasets in Muara Karang.

	Wind Speed (m/s)	Temperature (C)	Humidity (%)	Solar Irradiance (kWh/m^2/day)
max	6.86	28.88	93.44	7.46
min	0.52	24.03	63.58	0.81

4.2. Simulation results and discussions

Four prediction models based on machine learning, namely support vector machine (SVM) [34], least-square support vector machine (LS-SVM) [35], extreme learning machine (ELM) [36], and the proposed method called kernel extreme learning machine (K-ELM), were applied to the sample datasets. The comparisons of their performances in terms of MAE and speed of computation process are described in this section. The parameters of the four prediction models are provided in Table 3.

Table 3. Parameters of SVM, LS-SVM, ELM, and K-ELM.

SVM	LS-SVM	ELM	K-ELM
C = 0.0009	C = 0.0009	Hidden Neuron = 50	C = 10
σ = 15	σ = 15		σ = 50

The ELM learning algorithm utilized the RBF as the activation function, whereas SVM, LS-SVM, and K-ELM used the RBF as the kernel function. The real data record for solar irradiance data and the training process results are provided in Fig. 4. The highest errors in the training process produced by the K-ELM method were 3.97% and 4.12% for Lamongan and Muara Karang Areas respectively, as depicted in Fig. 5. The second-highest errors were obtained by ELM with 3.67% and 3.85%. The third-highest errors were obtained by LS-SVM with 1.44% and 0.29%. The lowest error values were obtained by the SVM approach with 0.47% and 0.13 for Lamongan and Muara Karang regions, respectively. These conditions occurred because the meteorological and solar irradiance variations in Lamongan and Muara Karang areas have non-linear characteristics and greatly affect the forecasting process.

The main objective of the training phase is to acquire the parameters of the proposed algorithm; thus, its parameter was utilized for the testing phase to test the efficacy of proposed method. The testing results of the forecaster model are depicted in Fig. 6. As shown in Fig. 7, the predictive accuracy criterion of the prediction scheme of the proposed method for the testing phase is better than those of ELM, LS-SVM, and SVM. The lowest MAE of Lamongan and Muara Karang areas is attained by proposed K-ELM with 0.6669, and 0.791, respectively. It is followed by ELM with 0.807 and 0.8001. The LS-SVM has MAE value of 1.2492 and 1.4315. The poorest result was found in SVM with 4.9829 and 4.6398 of MAE in Lamongan area and Muara Karang region, respectively.

Regarding the CPU time as described in Fig. 8(a)-(b) for the training phase, the proposed method has the best CPU time performance with 0.21 and 0.21 seconds for Lamongan and Muara Karang datasets, respectively. The second-best CPU time performance was obtained by ELM with 0.81 and 0.23 seconds. The third-best CPU time performance was attained by LS-SVM with 6.23 and 8.05 seconds. The poorest CPU time performance was obtained SVM with 18.17 and 20.56 seconds. The appropriately chosen data inputs of the learning algorithm play a key role in solar irradiation forecasting. When the feature selections are unrelated to the predicted response, the understanding of the relationship between them is disturbed and encourages long-term observation for the selection of features in the future. Simulation results have shown that the selection of features with little correlation will lead to a significant decrease in prediction accuracy.

For example, the learning algorithm model employed in this work has a good, predicted result for the training phase but produced an unsatisfactory forecasted result in the testing process.

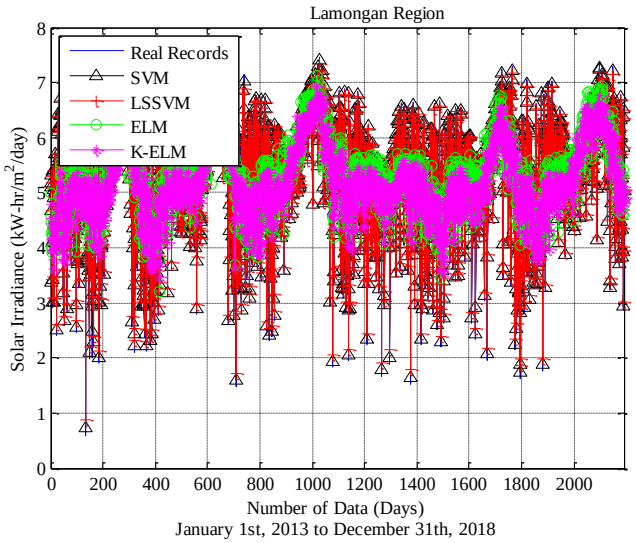

(a) Lamongan.

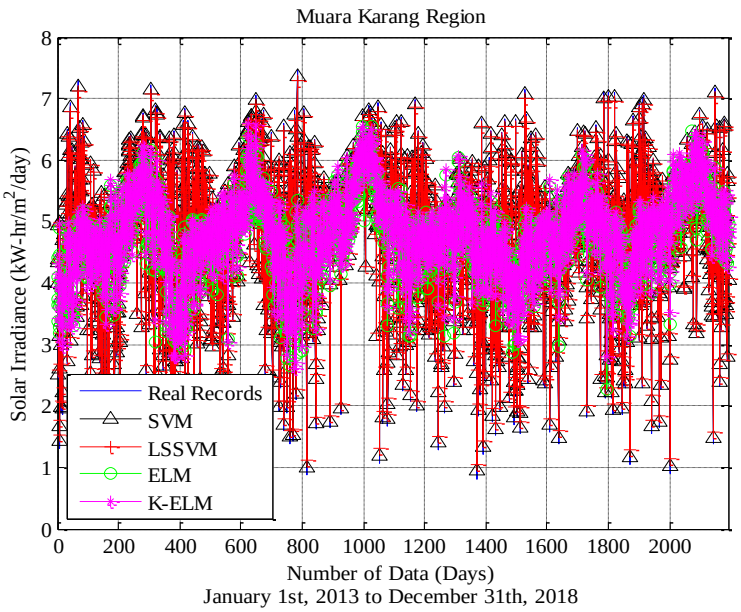

(b) Muara Karang.

Fig. 4. Training process results.

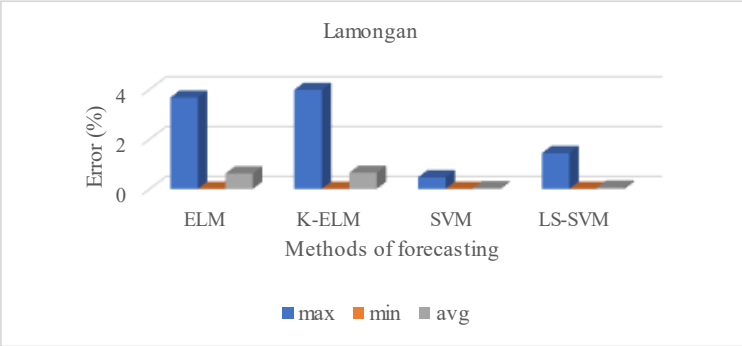

(a) Lamongan.

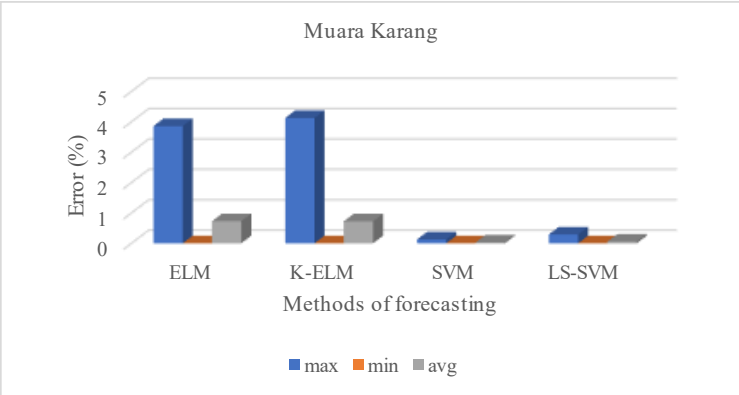

(b) Muara Karang.

Fig. 5. Maximum, minimum, and average values of error for training phase.

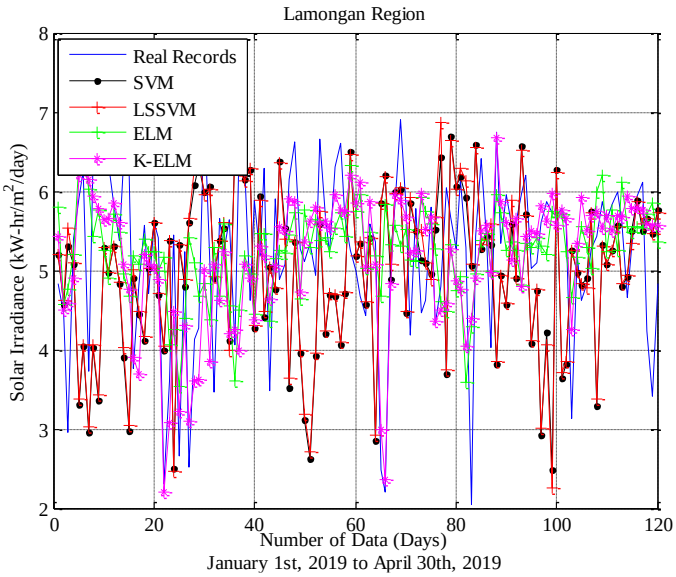

(a) Lamongan.

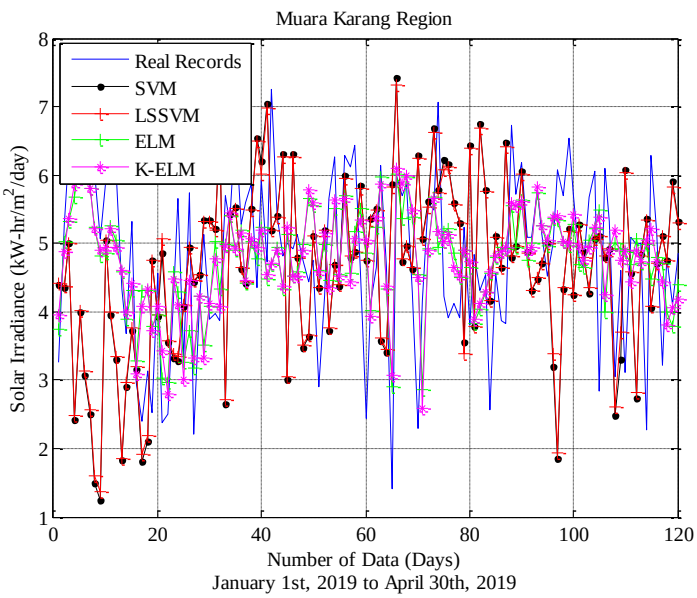

(b) Muara Karang.

Fig. 6. Testing phase results.

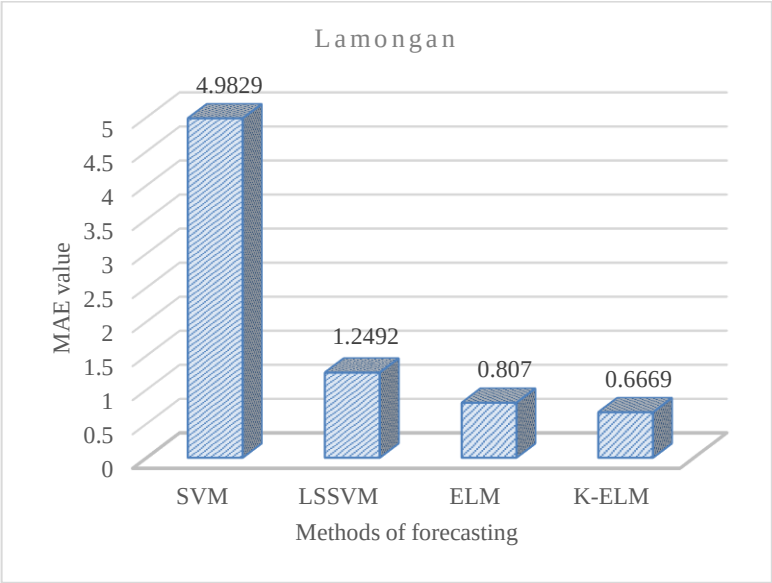

(a) Lamongan.

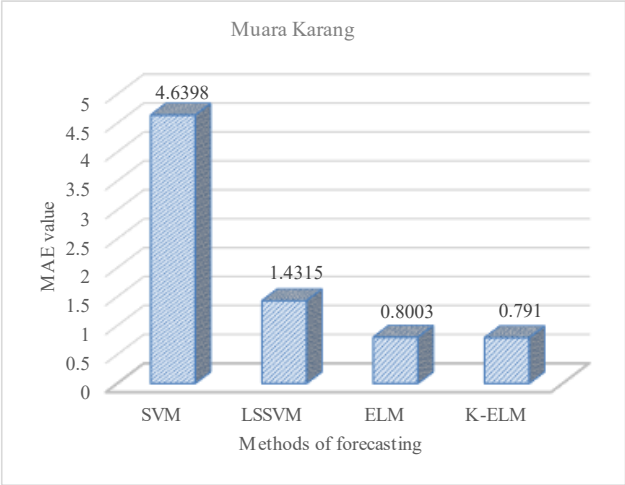

(b) Muara Karang.

Fig. 7. MAE values.

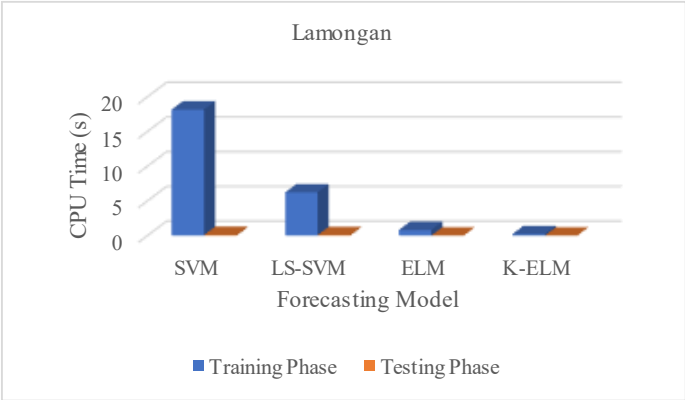

(a) Lamongan.

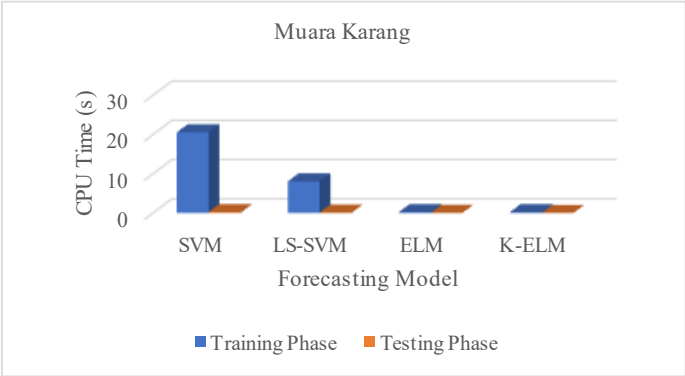

(b) Muara Karang.

Fig. 8. CPU times.

5. Conclusions

A new learning algorithm called K-ELM has been proposed to predict the solar irradiance in Lamongan and Muara Karang Areas, Indonesia in this paper. The simulation results show that the proposed approach has the lowest MAE value compared to those of the standard ELM, SVM, and LS-SVM for the testing phase. In terms of the learning speed, the proposed algorithm has the best performance compared to the other learning algorithms examined in this paper. The proposed algorithm achieves a more stable ability and better generalization performance than ELM, SVM, and LS-SVM algorithms in terms of learning speed. For the further study in the future, the application of a meta-heuristic approach to improving the performance of the learning algorithm might be necessary since the parameters of the present proposed learning algorithm are not optimized.

Acknowledgement

The research work was sponsored by UP-UTP research grant between Universitas Pertamina (UP), Indonesia, and Universiti Teknologi Petronas (UTP), Malaysia.

Nomenclatures

$\beta = [\beta_1, \beta_2, \dots, \beta_M]$	The output weights of the M neuron between an output neuron and a hidden layer
$h(x) = [h_1(x), h_2(x), \dots, h_M(x)]$	The hidden layer output regarding to input x
T	Predicted output
C	Regularization coefficient
H	Hidden layer output
O= HH^T and $\Omega(x, y)$	Kernel function of hidden neurons of ELM.
σ	Kernel parameter
X_n	The normalized data
X_p	The original data
$X_{p\text{-}min}$	The minimum values of datasets
$X_{p\text{-}max}$	The maximum values of datasets
X	The data of wind speed, temperature, humidity, and solar irradiance.
X_d	The denormalized data
N	The number of data
$\hat{y}_i$	The predicted data of K-ELM
y_i	The real data record

References

1. Mardlijah; Zhai G.; Adzkiya D.; Mardianto L.; and Ikhwan, M. (2019). Modified T2FSMC approach for solar panel systems. *Systems Science & Control Engineering*, 7(2), 189-197.
2. Alireza Z.; Baseer M.A.; and Saidur R. (2018). Application of support vector machine models for forecasting solar and wind energy resources: A review. *Journal of Cleaner Production*, 199(1), 272-285.

3. Rahul G.M.; Siddharth C.; and Basharat J. (2021). Development of global solar radiation models: A comprehensive review and statistical analysis for Indian regions. *Journal of Cleaner Production*, 293(1), 126208.
4. Yong Z.; Yanfeng L.; Dengjia W.; Xiaojun L.; and Yingying W. (2021). A review on global solar radiation prediction with machine learning models in a comprehensive perspective. *Energy Conversion and Management*, 235(1), 113960.
5. Qimeng C.; Yan L.; Kailin L.; Ying Y.; Danny H.W.L.; and Liu Y. (2020). Solar radiation zoning and daily global radiation models for regions with only surface meteorological measurements in China. *Energy Conversion and Management*, 225(1), 113447.
6. Yakoubi H.; EL Mghouchi Y.; Abdou N.; Hajou A.; and Khellouki. A. (2021). Correlating clearness index with cloud cover and other meteorological parameters for forecasting the global solar radiation over Morocco. *Optik*, 242(1), 167145.
7. Mihalakakou G.; Santamouris M.; and Asimakopoulos D.N. (2000). The total solar radiation time series simulation in Athens, using neural networks. *Theoretical and Applied Climatology*, 66(3-4), 185-197.
8. Victor H.Q.; Javier A.; Javier A.A.; and Laurel S. (2017). ANFIS, SVM and ANN soft-computing techniques to estimate daily global solar radiation in a warm sub-humid environment. *Journal of Atmospheric and Solar-Terrestrial Physics*, 155(1), 62-70.
9. Kamadinata J.O.; Ken T.L.; and Suwa T. (2019). Sky image-based solar irradiance prediction methodologies using artificial neural networks. *Renewable Energy* 134(1), 837-845.
10. Walch A.; Castello R.; Mohajeri N.; Guignard F.; Kanevski M.; and Scartezzini, J.L. (2019). Spatio-temporal modelling and uncertainty estimation of hourly global solar irradiance using Extreme Learning Machines. *Energy Procedia*, 158(1), 6378-6383.
11. Haixiang Z.; Ling L.; Li S.; Lilin C.; Zhinong W.; and Guoqiang S. (2020). Short-term global horizontal irradiance forecasting based on a hybrid CNN-LSTM model with spatiotemporal correlations. *Renewable Energy*, 160(1), 26-41.
12. Sara P.; Paulo C.; Rui S.; and Maria J.C. (2019). Development of an ANN based corrective algorithm of the operational ECMWF global horizontal irradiation forecasts. *Solar Energy*, 185(1), 387-405.
13. Billel A.; Antonio M.G.O.; Pedro A.G.; Rabah D.; Cesar H.M.; and Kahina D. (2021). A novel approach for global solar irradiation forecasting on tilted plane using hybrid evolutionary neural networks. *Journal of Cleaner Production*, 287(1), 125577.
14. Hai L.; Chi Z.; Ying-Yi H.; Yin H.; and Shuli W. (2019). Day-ahead spatiotemporal solar irradiation forecasting using frequency-based hybrid principal component analysis and neural network. *Applied Energy*, 247(1), 389-402.
15. Ying-Yi H.; John J.F.M.; and Arnel C.F. (2020). Day-ahead solar irradiation forecasting utilizing gramian angular field and convolutional long short-term memory. *IEEE Access*, 8(1), 18741-18753.

16. Sahbi B.; Mohamed B.; Adel M.; Ayoub L.; Omar K.; and Lioua K. (2021). Deep neural networks for predicting solar radiation at Hail Region, Saudi Arabia. *IEEE Access*, 9(1), 36719-36729.
17. Yuqing Z.; Bintao S.; and Weifang S. (2020). A tool condition monitoring method based on two-layer angle kernel extreme learning machine and binary differential evolution for milling. *Measurement*, 166(1), 108186.
18. Ping Y.; Dan W.; Wen-Bing Z.; Li-Hua F.; Jin-Lian D.; and Hang S. (2021). Ensemble of kernel extreme learning machine based random forest classifiers for automatic heartbeat classification. *Biomedical Signal Processing and Control*, 63(1), 102138.
19. Muhammad A.K.; Seifedine K.; Yu-Dong Z.; Tallha A.; Muhammad S.; Amjad R.; and Tanzila S. (2021). Prediction of COVID-19-pneumonia based on selected deep features and one class kernel extreme learning machine, *Computers & Electrical Engineering*, 90(1), 106960.
20. Ying Z.; Yuelei L.; Da F.; Jingpeng S.; and Fan Y. (2021). Application of kernel extreme learning machine and kriging model in prediction of heavy metals removal by biochar. *Bioresource Technology*, 329(1), 124876.
21. Bing L.; and Yong-Ping Z. (2020). Group reduced kernel extreme learning machine for fault diagnosis of aircraft engine. *Engineering Applications of Artificial Intelligence*, 96(1), 103968.
22. Lei C.; and Shuting W. (2021). Intelligent fault diagnosis of high-voltage circuit breakers using triangular global alignment kernel extreme learning machine. *ISA Transactions*, 109(1), 368-379.
23. Li W.; Meng J.E; and Shi Z. (2020). A kernel extreme learning machines algorithm for node localization in wireless sensor networks. *IEEE Communications Letters*, 24(7), 1433-1436.
24. Ning L.; Fuxing H.; Wentao M.; Ruotong W.; and Xiaoping Z. (2020). Wind power prediction of kernel extreme learning machine based on differential evolution algorithm and cross validation algorithm. *IEEE Access*, 8(1), 68874-68882.
25. Jiexiong T.; Chenwei D.; and Guang B.H. (2016). Extreme learning machine for multilayer perceptron. *IEEE Transactions on Neural Networks and Learning Systems*, 27(4), 809-821.
26. Huang G.B.; Wang D.H.; and Lan Y. (2011). Extreme learning machines: a survey. *International Journal of Machine Learning and Cybernetics*, 2(2), 107-122.
27. Waqar A.K.; Hoi-Lam M.; Xu O.; and Daniel Y.M. (2021). Prediction of aircraft trajectory and the associated fuel consumption using covariance bidirectional extreme learning machines. *Transportation Research Part E: Logistics and Transportation Review*, 145(1), 102189.
28. Siwar Y.; Salwa S.; and Mourad Z. (in press). Wavelet extreme learning machine and deep learning for data classification. *Neurocomputing*, 470, 280-289.
29. Ghalib A.T.; and Chu K.L. (2020). An open-ended continual learning for food recognition using class incremental extreme learning machines. *IEEE Access*, 8(1), 82328-82346.
30. Tassadaq H.; Sabato M.S.; Hsiao L.S.W.; Yu T.; Valerio M.S.; and Wen H.L. (2020). Ensemble hierarchical extreme learning machine for speech dereverberation, *IEEE Transactions on Cognitive and Developmental Systems*, 12(4), 744-758.

31. Li W.; Meng J. E.; and Shi Z. (2020). A kernel extreme learning machines algorithm for node localization in wireless sensor networks, *IEEE Communications Letters*, 24(7), 1433-1436.
32. Power Data Access Viewer (2020). Retrieved October 5, 2020, from https://power.larc.nasa.gov/data-access-viewer/.
33. MATLAB, MathWorks (2020). Retrieved October 8, 2020, from https://www.mathworks.com/products/matlab.html.
34. Jose M. A.A.; Jose G.R.M.; Saul A.O.B.; Guillermo R.L.; Eusebio V.R.; and Mario T.P. (2021). Hybrid techniques to predict solar radiation using support vector machine and search optimization algorithms: a review. *Applied Science*, 11(1), 1044.
35. Zuhaila M.Y.; Nur A.S.; Nur F. A.A.; Hasmaini M.; and Norfishah A.W. (2020). Prediction of solar irradiance using grey wolf optimizer least square support vector machine. *Indonesian Journal of Electrical Engineering and Computer Science*, 17(1), 10-17.
36. Omer A.K.; Tuba T.A.; and Ismail A. (2021). Estimation of solar radiation using modern methods. *Alexandria Engineering Journal*, 60(1), 2447-2455.